



Published in final edited form as:

Circulation. 2014 April 1; 129(13): 1428–1439. doi:10.1161/CIRCULATIONAHA.113.004146.

## Endothelial Cell-Specific LKB1 Deletion Causes Endothelial Dysfunction and Hypertension in Mice *in vivo*

Wencheng Zhang, PhD<sup>1</sup>, Qilong Wang, PhD<sup>1</sup>, Yue Wu, MD, PhD<sup>1,2</sup>, Cate Moriasi, PhD<sup>1</sup>, Zhaoyu Liu, MSc<sup>1,3</sup>, Xiaoyan Dai, PhD<sup>1</sup>, Qiongxin Wang, PhD<sup>1</sup>, Weimin Liu, MD<sup>2</sup>, Zu-Yi Yuan, MD, PhD<sup>2</sup>, and Ming-Hui Zou, MD, PhD<sup>1,2,4</sup>

<sup>1</sup>Section of Molecular Medicine, Department of Medicine, University of Oklahoma Health Sciences Center, Oklahoma City, OK

<sup>2</sup>Department of Cardiology, First Affiliated Hospital of Xi'an Jiaotong University Health Science Center, Xi'an, China

<sup>3</sup>Department of Biochemistry and Molecular Biology, University of Oklahoma Health Sciences Center, Oklahoma City, OK

<sup>4</sup>The Key Laboratory of Cardiovascular Remodeling and Function Research, Chinese Ministry of Education and Chinese Ministry of Public Health, Qilu Hospital of Shandong University, Jinan, Shandong, China

### Abstract

**Background**—Liver kinase B1 (LKB1), a tumor suppressor, is a central regulator of cell polarity and energy homeostasis. The role of LKB1 in endothelial function *in vivo* has not been explored.

**Methods and Results**—Endothelium-specific LKB1 knockout (*LKB1<sup>endo</sup>-/-*) mice were generated by crossbreeding *LKB1<sup>flox/flox</sup>* mice with VE-Cadherin-Cre mice. *LKB1<sup>endo</sup>-/-* mice exhibited hypertension, cardiac hypertrophy, and impaired endothelium-dependent relaxation. *LKB1<sup>endo</sup>-/-* endothelial cells exhibited reduced endothelial nitric oxide synthase (eNOS) activity and adenosine monophosphate-activated protein kinase (AMPK; downstream enzyme of LKB1) phosphorylation at Thr172, compared with those of wild-type (WT) cells. In addition, the levels of caveolin-1 were higher in the endothelial cells of *LKB1<sup>endo</sup>-/-* mice, and knockdown of caveolin-1 by siRNA normalized eNOS activity. Human antigen R (HuR) bound with the AU-rich elements of caveolin-1 mRNA 3' UTR, resulting in the increased stability of caveolin-1, and genetic knockdown of HuR decreased the expression of caveolin-1 in LKB1-deficient endothelial cells. Finally, adenoviral overexpression of constitutively active AMPK (CA-AMPK), but not green fluorescent protein (GFP), decreased caveolin-1, lowered blood pressure, and improved endothelial function in *LKB1<sup>endo</sup>-/-* mice *in vivo*.

**Conclusions**—Our findings indicate that endothelial LKB1 regulates eNOS activity, endothelial function, and blood pressure by modulating AMPK-mediated caveolin-1 expression.

### Keywords

LKB1; AMPK; caveolin-1; eNOS; hypertension

Correspondence: Ming-Hui Zou, MD, PhD, Department of Medicine, University of Oklahoma Health Science Center, Oklahoma City, OK 73104, Phone: 405-271-3974, Fax: 405-271-3973, ming-hui-zou@ouhsc.edu.

**Conflict of Interest Disclosures:** None.

## Introduction

The endothelium is a monocellular layer that covers the inner surface of blood vessels. It functions as a physical barrier that separates the circulating blood from the vascular walls. In addition, endothelial cells produce a wide range of factors that regulate vascular tone, cellular adhesion, thromboresistance, smooth muscle cell proliferation, and vessel wall inflammation.<sup>1</sup> In response to acetylcholine (ACh) and other physiological stimuli, the endothelium releases nitric oxide (NO) to trigger endothelium-derived vascular relaxation. Endothelial dysfunction is associated with major cardiovascular risk factors, such as aging, hyperhomocysteinemia, post-menopause, smoking, diabetes, hypercholesterolemia, and hypertension.<sup>2, 3</sup> However, a causative link between endothelial dysfunction and hypertension remains to be established. NO is a free radical gas that is generated from the metabolism of L-arginine by endothelial NO synthase (eNOS) in endothelial cells. It is the most important factor for maintaining normal endothelial function.<sup>4</sup> The essential role of eNOS-derived NO in the cardiovascular system is best demonstrated in eNOS knockout mice, which exhibit hypertension,<sup>5</sup> increased vascular smooth muscle cell proliferation in response to vessel injury,<sup>6</sup> increased leukocyte-endothelial interactions,<sup>7</sup> hypercoagulability,<sup>8</sup> and increased diet-induced atherosclerosis.<sup>9</sup> eNOS is functionally inhibited through the binding of a 20-amino-acid region of caveolin-1 (amino acids 82–101), called the caveolin-scaffolding domain.<sup>10</sup> Thus, caveolin-1 acts as an “inhibitory clamp” that keeps eNOS inactive.<sup>11</sup> The physiological significance of this regulation of eNOS by caveolin-1 is evident in caveolin-1 knockout mice, which are unable to regulate eNOS properly and, therefore, do not establish normal endothelium-dependent vascular tone.<sup>12, 13</sup> Although the regulation of eNOS by caveolin-1 is well-established, the upstream signaling components that regulate caveolin-1 expression remain unclear.

Liver kinase B1 (LKB1) is a serine/threonine protein kinase that was first described as a tumor suppressor gene, which is mutated in Peutz-Jeghers syndrome.<sup>14, 15</sup> LKB1 is ubiquitously expressed in mammalian cells, and it is activated in a complex with two scaffolding proteins: STE20-related adaptor protein and mouse protein 25.<sup>16</sup> Currently, LKB1 is implicated as a central regulator of cell polarity and energy metabolism in a variety of systems, through its ability to phosphorylate and activate the adenosine monophosphate-activated protein kinase (AMPK) family of proteins, which consists of 14 members.<sup>17</sup> Further roles of LKB1 have been identified through the production of LKB1 knockout mouse models. Global knockouts of LKB1 are embryonically lethal with major defects in cardiovascular developments, indicating that LKB1 has important functions in the cardiovascular system.<sup>18</sup> Dr. Mäkelä's group crossbred *LKB1<sup>flox/flox</sup>* mice with Tie1-Cre mice, and they discovered that the homozygous ablation of LKB1 with the Tie1 promoter results in embryonic lethality due to vascular disruption.<sup>19</sup> Furthermore, the homozygous ablation of the LKB1 allele with Tie2-Cre produces no viable pups.<sup>20</sup> Because Tie1 and Tie2 are expressed in hematopoietic lineages and neurological tissues,<sup>21, 22</sup> whether the embryonic lethality with Tie1- or Tie2-specific Cre mice is due to LKB1 deficiency in endothelial cells or other Tie1/Tie2-expressing tissues remains unknown. Since VE-Cadherin-Cre (VE-CAD-Cre), unlike Tie1- or Tie2-Cre, is uniformly expressed in the endothelium of developing and quiescent vessels, with a very small percentage found in hematopoietic cells,<sup>23</sup> using VE-CAD-Cre would eliminate the effects of non-endothelial cell LKB1 deletion. Thus, the aim of the present study was to examine the roles of LKB1 in maintaining endothelial function and blood pressure without the effects of non-endothelial LKB1 in endothelium-specific LKB1 knockout mice (*LKB1<sup>endo-/-</sup>*) generated by crossing breeding *LKB1<sup>flox/flox</sup>* mice with VE-Cadherin-Cre mice. Here we report the endothelium-specific LKB1 deletion caused endothelial dysfunction and hypertension *in vivo*.

## Materials and Methods

### Animals

Mice expressing the Cre recombinase under control of the *VE-Cadherin* promoter/enhancer (VE-CAD-Cre) were purchased from Jackson Laboratory.<sup>23</sup> LKB1-floxed (*LKB1<sup>flox/flox</sup>*) mice were purchased from the National Cancer Institute, which was made by DePinho lab.<sup>24</sup> To generate endothelium-specific *LKB1<sup>endo-/-</sup>* mice, *LKB1<sup>flox/flox</sup>* mice were crossbred with VE-CAD-Cre mice. PCR-based genotyping was performed, as described previously.<sup>25</sup> The animals were housed in a controlled environment ( $20 \pm 2^\circ\text{C}$ , 12-h/12-h light/dark cycle), where they were maintained on a standard chow diet with free access to water. Male mice at 3 months of age were subjected to endothelial function analyses and blood pressure measurements. For adenoviral injections, wild-type (WT) or *LKB1<sup>endo-/-</sup>* mice received tail vein injections of 100  $\mu\text{L}$  adenoviral vectors that expressed green fluorescent protein (GFP) or constitutively active (CA)-AMPK ( $4 \times 10^{10}$  viral particles). The animal protocol was reviewed and approved by the Animal Care and Use Committee at the University of Oklahoma Health Sciences Center.

### Reagents

Antibodies to caveolin-1, phospho-AMPK $\alpha$  T172, AMPK $\alpha$ , Histone H3, eNOS, and phospho-eNOS Ser1177 were from Cell Signaling Technology (Danvers, MA). Antibodies to LKB1 and GAPDH were purchased from Santa Cruz Biotechnology (Santa Cruz, CA). Anti-HuR was purchased from Millipore (Temecula, CA). Anti-CD31 was from Abcam (Cambridge, UK). FuGene HD transfection reagent was from Roche Applied Science (Indianapolis, IN).

### Measurement of blood pressure

Blood pressure was measured using the radiotelemetry technique, as described previously.<sup>26</sup> Mice were anesthetized with a ketamine and xylazine mixture (70:6 mg/kg, intraperitoneal injection). The left common carotid artery was exposed, and a catheter (PE10 tubing) was inserted. The body of the telemetry transmitter unit (TA11PA-C10; Data Sciences International, St. Paul, MN) was then inserted under the skin, and the signal was received and recorded by the data acquisition program (Dataquest ART 3.1, Data Sciences).

### Measurement of vessel tension in mice

Aortas or mesenteric arteries were immersed in Krebs bicarbonate buffer (118 mM NaCl, 4.7 mM KCl, 25 mM NaHCO<sub>3</sub>, 1.2 mM KH<sub>2</sub>PO<sub>4</sub>, 1.2 mM MgSO<sub>4</sub>, 2.5 mM CaCl<sub>2</sub>, and 5 mM glucose) and then suspended by two tungsten wires mounted in a vessel myograph system (Danish Myotechnologies, Aarhus, Denmark). After undergoing an equilibration period, rings were treated with phenylephrine (PE) for induction of contraction. To study vasodilator and L-nitro arginine methyl ester (L-NAME) responses, the rings were precontracted with PE, and acetylcholine (ACh) ( $10^{-10}$  to  $10^{-4}$  M), sodium nitroprusside (SNP) ( $10^{-10}$  to  $10^{-5}$  M), or L-NAME (100  $\mu\text{M}$ ) was injected at the plateau of the PE-induced contraction.

### Assays of eNOS activity

eNOS activity was detected by measuring the conversion of [<sup>3</sup>H] L-arginine to [<sup>3</sup>H] L-citrulline with the eNOS assay kit (Cayman) according to the manufacturer's instructions. Protein concentration was determined with the BCA Assay Kit (Pierce Chemical Co., Rockford, Illinois, USA). eNOS activity was expressed as pmol L-citrulline/mg protein/min. All samples were assayed in triplicate.

## RNA immunoprecipitation (IP) assays

Magna RIP™ kit (Cat 17-700, Millipore) was used for RNA IP assays according to the manufacturer's instructions. Briefly, whole-cell lysates were incubated at 4°C overnight with magnetic protein A/G beads previously precoated with 5 µg of either rabbit IgG or HuR antibody (Millipore). Beads were washed and incubated with proteinase K buffer (30 min, 55°C) followed by RNA isolation from the immunoprecipitates and subsequently cDNA synthesis. PCR was performed by using of the following primers: caveolin-1-F: 5'-CTACAAGCCCAACAACAAGGC-3' and R: 5'-AGGAAGCTCTTGATGCACGGT-3'. Cyclooxygenase-2-F: 5'-AACCGCATTGCCTCTGAAT-3' and R: 5'-CATGTTCCAGGAGGATGGAG-3'.

## Statistical Analysis

Data are presented as means ± standard error of the mean (SEM), and the results were analyzed with GraphPad Prism (GraphPad Software Inc., San Diego, CA). After confirming the normal distribution using the Kolmogorov-Smirnov test, statistical comparisons were made with the Student t test for unpaired data and ANOVA followed by the Bonferroni post hoc test when appropriate. Assuming  $\alpha = 0.05$ ,  $\beta = 0.90$ , and a ratio of (expected effect size)/(expected standard deviation) = 1.20, an  $n$  of at least 10 samples per group was required. Groups were considered to be significantly different at  $p$  values < 0.05.

A detailed description of other methods used in this study can be found in the online supplement.

## Results

### Generation and Analysis of *LKB1<sup>endo-/-</sup>* Mice

To elucidate the biological significance of LKB1 expression in vascular endothelial cells *in vivo*, VE-CAD-Cre mice were crossbred with *LKB1<sup>flox/flox</sup>* mice to generate VE-CAD-Cre/*LKB1<sup>flox/+</sup>* mice. These were further intercrossed to obtain VE-CAD-Cre/*LKB1<sup>flox/flox</sup>* mice (referred to as *LKB1<sup>endo-/-</sup>*) (Figure 1A). The littermate *LKB1<sup>flox/flox</sup>/Cre<sup>-</sup>* mice were used as WT controls.

A total of 851 mice were generated from 40 litters of crosses between VE-CAD-Cre/*LKB1<sup>flox/+</sup>* mice. Analysis of the resulting genotypes revealed a lower Mendelian frequency for *LKB1<sup>endo-/-</sup>* mice (5.6% shown versus 25.0% expected, Figure 1B). Other *LKB1<sup>endo-/-</sup>* mice died before birth; this was consistent with previous findings.<sup>19</sup> *LKB1<sup>endo-/-</sup>* mice that survived into adulthood were indistinguishable from their control littermates and were used for subsequent experiments.

To confirm endothelium-specific LKB1 deletion in *LKB1<sup>endo-/-</sup>* mice, immunofluorescence was used to detect LKB1 expression in the aortas that were isolated from these mice. Endothelial cells were detected via CD31 staining. LKB1 was expressed in the endothelium and smooth muscle of aortas from WT mice, but not in the endothelium from *LKB1<sup>endo-/-</sup>* mice (Figure 1C). To confirm the efficiency of LKB1 knockout in endothelial cells, we isolated mouse lung endothelial cells (MLECs) from the mice. LKB1 was barely detectable in MLECs from *LKB1<sup>endo-/-</sup>* mice, thus confirming effective LKB1 deletion in *LKB1<sup>endo-/-</sup>* mice (Figure 1D).

### Elevated blood pressure and cardiac hypertrophy in *LKB1<sup>endo-/-</sup>* mice

To characterize the phenotypes of *LKB1<sup>endo-/-</sup>* mice, we evaluated blood pressure using the radiotelemetry technique. As shown in Figure 2A, both the diastolic blood pressure (112 ± 11 mm Hg versus 83 ± 8 mm Hg) and the systolic blood pressure (148 ± 8 mm Hg versus

117 ± 9 mm Hg) are significantly higher in *LKB1<sup>endo-/-</sup>* mice, compared with their WT littermates. Consequently, *LKB1<sup>endo-/-</sup>* mice had higher mean blood pressure (mBP) (125 ± 8 mm Hg) than that of WT mice (94 ± 8 mm Hg). Similarly, the ratios of heart weight to body weight in *LKB1<sup>endo-/-</sup>* mice were significantly greater than those in their WT littermates (Figure 2B and 2C). Morphometric analysis of the hearts from *LKB1<sup>endo-/-</sup>* mice showed that both the left and right ventricular walls were enlarged (Figure 2D), which was consistent with a hypertrophic response. Collectively, these results show that LKB1 deficiency in the endothelium resulted in elevated blood pressure and cardiac hypertrophy.

### Endothelial deletion of LKB1 impairs eNOS-dependent vasodilation

The vascular contractile response is an important peripheral component of the blood pressure regulatory system. Given the increased blood pressure in *LKB1<sup>endo-/-</sup>* mice, we examined the effect of endothelial LKB1 deletion on vascular function. As shown in Figure 3A, there is no significant change in the phenylephrine (PE) (10<sup>-6</sup> M)-induced contraction force between the aortas from WT (6.46 ± 0.72 mN) and *LKB1<sup>endo-/-</sup>* mice (6.28 ± 1.27 mN). When PE-induced contractions reached a plateau, increasing doses of acetylcholine (ACh; 10<sup>-10</sup> to 10<sup>-4</sup> M) were added. ACh-induced relaxations in WT aortas were concentration-dependent. However, ACh-induced relaxations were significantly reduced in *LKB1<sup>endo-/-</sup>* aortas (Figure 3B). Interestingly, ACh elicited similar responses in the two strains when the aortas were pretreated with an eNOS inhibitor (L-NAME, 10<sup>-4</sup> M) for 30 min (Figure 3C). These results indicate that the impaired vasorelaxation in the *LKB1<sup>endo-/-</sup>* aorta is eNOS-mediated. In contrast, relaxations caused by sodium nitroprusside (SNP), which is an endothelium-independent agent, did not significantly differ between WT and *LKB1<sup>endo-/-</sup>* mice (Figure 3D), indicating that LKB1 deficiency only affects endothelial function in *LKB1<sup>endo-/-</sup>* mice. Using mesenteric vessels to further confirm this phenotype, we found that vessels from *LKB1<sup>endo-/-</sup>* mice were less responsive to ACh (Figure 3E), and pretreatment with L-NAME elicited similar levels of responsiveness (Figure 3F). Basal NO release in *LKB1<sup>endo-/-</sup>* mice was also reduced (Figure 3G). Additionally, vessels were pre-constricted with a submaximal dose of PE (10<sup>-7</sup> M), and L-NAME (10<sup>-4</sup> M) was added at the peak of constriction to remove endogenous NO, which caused further constriction of the WT vessels (3.53 ± 0.76 mN). However, constriction of the vessels in response to L-NAME was significantly attenuated in *LKB1<sup>endo-/-</sup>* mice (1.10 ± 0.46 mN) (Figure 3H). Overall, these data suggest that endothelial deletion of LKB1 impairs eNOS-dependent vasodilation.

### Decreased eNOS activity in *LKB1<sup>endo-/-</sup>* mice

To measure eNOS activity in lung tissues, we monitored the [<sup>3</sup>H] arginine-to-citrulline conversion. The activity of eNOS was decreased in *LKB1<sup>endo-/-</sup>* lung extracts (0.34 ± 0.08 pmol L-citrulline/mg protein/min), compared with that of WT (1.24 ± 0.20 pmol L-citrulline/mg protein/min) (Figure 4A). To understand how LKB1 regulates eNOS activity in endothelial cells, the protein levels of phosphorylated eNOS at Ser1177 (p-eNOS) and total eNOS were assessed via western blot analysis. There was no change in the levels of p-eNOS and total eNOS between WT and *LKB1<sup>endo-/-</sup>* endothelial cells, suggesting that LKB1 regulates eNOS activity through alternative signaling pathways (Figure 4B).

Caveolin-1 can bind to eNOS and inhibit its bioactivity by holding it in an inactive conformation.<sup>27,28</sup> Importantly, LKB1 deletion significantly increased caveolin-1 levels (Figure 4C). Although eNOS activity was much lower in *LKB1<sup>endo-/-</sup>* endothelial cells, siRNA knockdown of caveolin-1 significantly increased eNOS activity in both WT and *LKB1<sup>endo-/-</sup>* endothelial cells (Figure 4D). These data suggest that increased caveolin-1 contributes to the decrease in eNOS activity in *LKB1<sup>endo-/-</sup>* endothelial cells.



To investigate whether the association of eNOS with caveolin-1 can blunt AMPK-induced eNOS phosphorylation, human umbilical vein endothelial cells (HUVECs) were transfected with control siRNA or caveolin-1 siRNA. Forty-eight hours after transfection, HUVECs were incubated with AICAR (2 mM) for 30 min. As shown in Supplementary Figure 1, AICAR induces eNOS phosphorylation at Ser1177 at similar levels in both control siRNA- and caveolin-1 siRNA-transfected HUVECs. This suggests that the association of eNOS with caveolin-1 does not alter the ability of AMPK to phosphorylate eNOS at Ser1177.

### Increased expression of caveolin-1 in the endothelium of *LKB1<sup>endo-/-</sup>* mice

Compared with WT mice, caveolin-1 expression was significantly increased in the endothelium of *LKB1<sup>endo-/-</sup>* mice (Figure 5A). Moreover, *LKB1<sup>endo-/-</sup>* endothelial cells exhibited a 1.86-fold increase in caveolin-1 mRNA levels (Figure 5B). In *LKB1<sup>endo-/-</sup>* lung extracts, increased co-immunoprecipitation of caveolin-1 and eNOS was observed (Figure 5C & 5D), thus confirming that they associate with each other. These data suggest that LKB1 deletion in the endothelium results in the aberrant overexpression of caveolin-1, and the association of caveolin-1 with eNOS.

### Caveolin-1 is a target of human antigen R (HuR)

To better understand the regulation of caveolin-1 expression by LKB1, we examined its 5'UTR and 3'UTR to assess whether caveolin-1 may be a target of post-transcriptional modification. We identified four conserved AU-rich elements (AREs) in the 3'UTR of caveolin-1 mRNA (Figure 6A). HuR is an RNA-binding protein that regulates the stability of ARE-containing transcripts, and AMPK activation can inhibit HuR translocation from the nucleus to the cytosol.<sup>29</sup> Therefore, we evaluated the effect of LKB1 deletion on HuR translocation. As depicted in Figure 6B, *LKB1<sup>endo-/-</sup>* endothelial cells have elevated cytoplasmic HuR levels, although LKB1 deletion does not alter total HuR levels (Supplementary Figure 2).

The ability of HuR to bind with the 3'UTR of caveolin-1 mRNA was also assessed. RNA immunoprecipitation with either an anti-HuR antibody or control IgG showed that HuR binds to caveolin-1 mRNA (Figure 6C). Cyclooxygenase-2, a known target of HuR, was used as a positive control in this assay. To map out the HuR binding site in the 3'UTR of caveolin-1 mRNA, we used an RNA pull-down assay, where biotinylated RNA probes that corresponded to the fragments depicted in Figure 6A were incubated with endothelial cell extracts. GAPDH 3'UTR and Myc 3'UTR probes were used as the negative and positive controls, respectively. HuR was pulled down with the probe that contained the second ARE (Figure 6D), suggesting that the second ARE within the 3' UTR of caveolin-1 is necessary for its association with HuR. Next, we examined the effects of HuR on the stability of endogenous caveolin-1 mRNA. Endothelial cells were transfected with HuR or LacZ plasmids and then treated with actinomycin D, a transcriptional inhibitor. The half-life of caveolin-1 mRNA was increased from 6.5 h to 10 h after HuR transfections (Figure 6E), indicating that HuR enhances caveolin-1 mRNA stability.

Interestingly, HuR knockdown with siRNA suppressed caveolin-1 expression in WT and *LKB1<sup>endo-/-</sup>* cells (Figure 6F). This suggests that HuR binds to and stabilizes endogenous caveolin-1 mRNA transcripts, thus resulting in elevated caveolin-1 protein levels.

### LKB1 regulates caveolin-1 expression in an AMPK-dependent manner

Because AMPK is a well-characterized substrate of LKB1, we monitored the phosphorylation of AMPK $\alpha$  (Thr172) in MLECs from WT or *LKB1<sup>endo-/-</sup>* mice. Phosphorylated AMPK (p-AMPK) was significantly decreased in *LKB1<sup>endo-/-</sup>* cells (Figure 7A). To determine whether the regulation of caveolin-1 by LKB1 was mediated through

AMPK, MLECs were treated with AICAR or Compound C (CpC; AMPK inhibitor) for 48 hours. AMPK activation with AICAR decreased caveolin-1 expression, whereas AMPK inhibition with CpC increased the levels of caveolin-1 (Figure 7B).

To further confirm the inverse relationship of caveolin-1 and AMPK, immunohistochemical staining was employed to evaluate the levels of caveolin-1 in the aortas from *AMPK $\alpha$ 1<sup>-/-</sup>* or *AMPK $\alpha$ 2<sup>-/-</sup>* mice. Caveolin-1 levels were markedly elevated in the endothelial cell layers in the aortas of *AMPK $\alpha$ 1<sup>-/-</sup>* or *AMPK $\alpha$ 2<sup>-/-</sup>* mice (Figure 7C).

To examine the effect of AMPK on HuR binding with caveolin-1 mRNA, AMPK $\alpha$  was silenced with AMPK $\alpha$ -specific siRNA, followed by RNA immunoprecipitation with IgG or the HuR antibody. Caveolin-1 mRNA was significantly enriched in the HuR immunoprecipitate, relative to the IgG control, and AMPK $\alpha$  knockdown further increased HuR enrichment with caveolin-1 mRNA (Figure 7D). These results indicate that AMPK regulates caveolin-1 expression through HuR.

To confirm the role of AMPK in the regulation of caveolin-1 and eNOS activity, eNOS expression and activity were assayed in lung endothelial cells that were isolated from *AMPK $\alpha$ 1<sup>-/-</sup>* or *AMPK $\alpha$ 2<sup>-/-</sup>* mice. Although AMPK $\alpha$ 1 was the main isoform in the endothelium (Figure 7E), the levels of caveolin-1 in endothelial cells from either *AMPK $\alpha$ 1<sup>-/-</sup>* or *AMPK $\alpha$ 2<sup>-/-</sup>* mice were markedly higher than those in WT mice (Figure 7F). Consistently, eNOS activities in *AMPK $\alpha$ 1<sup>-/-</sup>* or *AMPK $\alpha$ 2<sup>-/-</sup>* endothelial cells were significantly lower than those in WT mice (Figure 7G). As expected, endothelial cells from *LKB1<sup>endo</sup>-/-* mice exhibited higher levels of caveolin-1. Consistently, eNOS activity in *LKB1<sup>endo</sup>-/-* mice was markedly lower than that from *AMPK $\alpha$ 1<sup>-/-</sup>* or *AMPK $\alpha$ 2<sup>-/-</sup>* mice (Figure 7F & 7G).

The effect of adenoviral overexpression of CA-AMPK on the expression of caveolin-1 in endothelial cells from *LKB1<sup>endo</sup>-/-* mice was also determined. As shown in Figure 7H, adenoviral overexpression of CA-AMPK, but not the virus-encoded GFP, suppresses caveolin-1 expression in *LKB1<sup>endo</sup>-/-* endothelial cells (Figure 7H).

### Administration of CA-AMPK alleviates endothelial dysfunction and lowers high blood pressure in *LKB1<sup>endo</sup>-/-* mice

The administration of CA-AMPK increased the phosphorylation of AMPK $\alpha$  (T172) in the vascular endothelium of WT and *LKB1<sup>endo</sup>-/-* mice (Figure 8A). A decrease in the mBP of *LKB1<sup>endo</sup>-/-* mice was observed after three days, whereas the adenoviral administration of GFP had no effect (Figure 8B). The administration of CA-AMPK did significantly lower the mBP of *LKB1<sup>endo</sup>-/-* mice (*LKB1<sup>endo</sup>-/-* + CA-AMPK:  $102 \pm 8$  mm Hg versus *LKB1<sup>endo</sup>-/-* + GFP:  $124 \pm 7$  mm Hg) (Figure 8C). Similarly, CA-AMPK administration decreased the mBP of WT mice to  $82 \pm 8$  mm Hg, compared with  $95 \pm 11$  mm Hg in GFP-treated WT mice (Figure 8B and 8C). ACh-induced endothelial relaxation responses in both *LKB1<sup>endo</sup>-/-* and WT mice were also significantly improved with CA-AMPK administration (Figure 8D). Our data indicate that AMPK plays an important role in the LKB1-mediated regulation of endothelial function and blood pressure.

## DISCUSSION

This study is the first to show that endothelium-specific LKB1 deletion decreases eNOS activity and impairs endothelial function, resulting in hypertension and cardiac hypertrophy. In *LKB1<sup>endo</sup>-/-* endothelial cells, knockdown of caveolin-1 with siRNA normalized eNOS activity, genetic knockdown of HuR decreased caveolin-1 levels, and overexpression of HuR increased the mRNA stability of caveolin-1. Finally, adenoviral overexpression of CA-

AMPK decreased caveolin-1, lowered blood pressure, and improved endothelial function in *LKB1<sup>endo-/-</sup>* mice *in vivo*. We conclude that LKB1 plays an essential role in mediating the expression of caveolin-1 via AMPK to maintain normal endothelial function and blood pressure (Figure 8E). To research the roles of LKB1 in the endothelium *in vivo*, several groups have attempted to develop endothelial cell-specific knockout mice by crossbreeding *LKB1<sup>flox/flox</sup>* mice with Tie1- or Tie2-Cre mice. However, the homozygous ablation of the LKB1 allele with Tie1- or Tie2-Cre produces no viable pups, due to vascular defects.<sup>19, 20</sup> This can be explained by the broad expression of Tie1/Tie2-Cre in hematopoietic lineages, neuronal populations, and the mesoderm.<sup>21, 22</sup> On the other hand, VE-CAD-Cre is more specifically expressed in endothelial cells.<sup>23</sup> Therefore, it appears to be a better model than Tie1 or Tie2 that can be used to study the functions of essential genes in endothelial cells. Indeed, a recent study reported that specifically deleting VEGF in endothelial cells using VE-CAD-Cre yields viable adult mice, although most of these mice die at various stages.<sup>30</sup> By crossbreeding *LKB1<sup>flox/flox</sup>* mice with *VE-CAD-Cre* mice, we were able to obtain sufficient numbers of *LKB1<sup>endo-/-</sup>* mice, although the ratio of *LKB1<sup>flox/flox</sup>: VE-CAD-Cre<sup>+</sup>* was only 5.6%. However, the reasons for the differences in viability between LKB1-VE-CAD-Cre mice and LKB1-Tie1-/Tie2-Cre mice are unknown and warrant further investigation.

Caveolin-1 is a multi-functional scaffolding protein with multiple binding partners that are associated with cell surface caveolae.<sup>31</sup> It has the ability to bind to and inactivate eNOS.<sup>11</sup> The most important finding of the present study is that LKB1 deletion leads to the aberrant expression of caveolin-1, which consequently suppresses eNOS activity and results in endothelial dysfunction, likely via AMPK. Mechanistically, we found that caveolin-1 is regulated by HuR via AMPK. Indeed, previous study<sup>29</sup> has demonstrated that AMPK activation inhibits the translocation of HuR from the nucleus to the cytosol through regulation of importin alpha1, an adaptor protein involved in nuclear import. First, AMPK triggered the acetylation of importin alpha1 on Lys22, a process dependent on the acetylase activity of p300. Second, AMPK phosphorylated importin alpha1 on Ser105.<sup>29</sup> Consistently, published studies from us and others have shown that the LKB1-AMPK signaling pathway is active in the vasculature. LKB1 in cultured endothelial cells activates AMPK in response to PKC $\zeta$  activation and the treatment of cultured endothelial cells with AICAR activates AMPK in an LKB1 dependent manner in cultured human umbilical vein endothelial cells (HUVECs).<sup>32,33</sup> Consistently, we found LKB1 deletion decreased the levels of p-AMPK Thr172 and increased the translocation of HuR into the cytoplasmic compartments, where HuR was bound to the 3' UTR of caveolin-1 mRNA, thus resulting in enhanced stability. HuR is known to bind to and stabilize critical ARE-containing mRNAs, such as PAI-2, VEGF, and p21,<sup>34-36</sup> to enhance translation. Our findings provide a new regulatory mechanism for caveolin-1 expression. Endothelial caveolin-1 plays an important role in the regulation of NO production and vascular permeability,<sup>37</sup> atherosclerosis,<sup>38</sup> and angiogenesis,<sup>39</sup> thus implying a role for LKB1-mediated caveolin-1 regulation in these processes. AMPK can mediate the function of eNOS via multiple mechanisms. Previous studies have demonstrated that eNOS phosphorylation and activation are AMPK-dependent in the presence of pharmacological agents and physiological stress.<sup>40-42</sup> However, there are also reports showing that AMPK activation by hypoxia, pentobarbital, and glucose deprivation does not increase eNOS phosphorylation,<sup>43,44</sup> suggesting a context-dependent regulation of eNOS by AMPK. In our study, LKB1 deletion in endothelial cells decreased phosphorylated AMPK $\alpha$  (T172) levels and eNOS activity, while p-eNOS levels remained unchanged, suggesting a novel mechanism by which AMPK regulates eNOS activity via HuR-mediated caveolin-1 expression.

Findings from this study may be clinically applicable in human diseases, in which the expression or activity of LKB1 or AMPK are reduced. Consistently, the expression or



activity of LKB1 is reduced in cardiac hypertrophy.<sup>45</sup> Furthermore, 4-hydroxy-trans-2-nonenal, which is a common reactive lipid oxidant that is elevated in many human diseases, directly inhibits LKB1 by binding to Lys-97.<sup>46</sup> In our study, we presented one mechanism that might be linked to hypertension in humans. However, patients with Peutz-Jeghers syndrome, a disease caused by LKB1 mutations, appear to be normotensive, implicating the need for total LKB1 deletion to induce the mechanism described in mice in this manuscript. Moreover, the hearts from *LKB1<sup>endo-/-</sup>* mice developed comparable left and right ventricular hypertrophy (Figure 2D), these results raise the possibility that beside systemic hypertension, *LKB1<sup>endo-/-</sup>* mice may have pulmonary hypertension. Further investigation on LKB1 contribution in pulmonary hypertension is warranted.

In summary, this study identifies a molecular mechanism by which LKB1 deficiency causes endothelial dysfunction and hypertension. The loss of LKB1 contributes to increased caveolin-1 expression and the subsequent suppression of eNOS activity, thereby adversely affecting endothelial function and blood pressure regulation. Since AMPK activation can effectively attenuate the effects of LKB1 deletion, AMPK might be a therapeutic target of anti-hypertension therapy.

## Supplementary Material

Refer to Web version on PubMed Central for supplementary material.

## Acknowledgments

**Funding Sources:** This study was supported by National Institutes of Health grants (HL074399, HL080499, HL089920, HL110488, and HL105157) and funds from the Warren Chair in Diabetes Research at the University of Oklahoma Health Science Center (all to M.Z.). M.Z. is a recipient of the National Established Investigator Award from the American Heart Association.

## References

1. Deanfield JE, Halcox JP, Rabelink TJ. Endothelial function and dysfunction: Testing and clinical relevance. *Circulation*. 2007; 115:1285–1295. [PubMed: 17353456]
2. Brunner H, Cockcroft JR, Deanfield J, Donald A, Ferrannini E, Halcox J, Kiowski W, Luscher TF, Mancia G, Natali A, Oliver JJ, Pessina AC, Rizzoni D, Rossi GP, Salvetti A, Spieker LE, Taddei S, Webb DJ. Endothelial function and dysfunction. Part II: Association with cardiovascular risk factors and diseases: A statement by the working group on endothelins and endothelial factors of the European Society of Hypertension. *J Hypertens*. 2005; 23:233–246. [PubMed: 15662207]
3. Versari D, Daghini E, Viridis A, Ghiadoni L, Taddei S. Endothelial dysfunction as a target for prevention of cardiovascular disease. *Diabetes Care*. 2009; 32:S314–321. [PubMed: 19875572]
4. Palmer RM, Ferrige AG, Moncada S. Nitric oxide release accounts for the biological activity of endothelium-derived relaxing factor. *Nature*. 1987; 327:524–526. [PubMed: 3495737]
5. Huang PL, Huang Z, Mashimo H, Bloch KD, Moskowitz MA, Bevan JA, Fishman MC. Hypertension in mice lacking the gene for endothelial nitric oxide synthase. *Nature*. 1995; 377:239–242. [PubMed: 7545787]
6. Moroi M, Zhang L, Yasuda T, Virmani R, Gold HK, Fishman MC, Huang PL. Interaction of genetic deficiency of endothelial nitric oxide, gender, and pregnancy in vascular response to injury in mice. *J Clin Invest*. 1998; 101:1225–1232. [PubMed: 9502763]
7. Lefer DJ, Jones SP, Girod WG, Baines A, Grisham MB, Cockrell AS, Huang PL, Scalia R. Leukocyte-endothelial cell interactions in nitric oxide synthase-deficient mice. *Am J Physiol*. 1999; 276:H1943–1950. [PubMed: 10362674]
8. Freedman JE, Sauter R, Battinelli EM, Ault K, Knowles C, Huang PL, Loscalzo J. Deficient platelet-derived nitric oxide and enhanced hemostasis in mice lacking the NOSIII gene. *Circ Res*. 1999; 84:1416–1421. [PubMed: 10381894]

9. Kuhlencordt PJ, Gyurko R, Han F, Scherrer-Crosbie M, Aretz TH, Hajjar R, Picard MH, Huang PL. Accelerated atherosclerosis, aortic aneurysm formation, and ischemic heart disease in apolipoprotein E/endothelial nitric oxide synthase double-knockout mice. *Circulation*. 2001; 104:448–454. [PubMed: 11468208]
10. Li S, Couet J, Lisanti MP. Src tyrosine kinases, Galpha subunits, and H-Ras share a common membrane-anchored scaffolding protein, caveolin. Caveolin binding negatively regulates the auto-activation of Src tyrosine kinases. *J Biol Chem*. 1996; 271:29182–29190. [PubMed: 8910575]
11. Carver LA, Schnitzer JE. Caveolae: Mining little caves for new cancer targets. *Nat Rev Cancer*. 2003; 3:571–581. [PubMed: 12894245]
12. Drab M, Verkade P, Elger M, Kasper M, Lohn M, Lauterbach B, Menne J, Lindschau C, Mende F, Luft FC, Schedl A, Haller H, Kurzchalia TV. Loss of caveolae, vascular dysfunction, and pulmonary defects in caveolin-1 gene-disrupted mice. *Science*. 2001; 293:2449–2452. [PubMed: 11498544]
13. Razani B, Engelman JA, Wang XB, Schubert W, Zhang XL, Marks CB, Macaluso F, Russell RG, Li M, Pestell RG, Di Vizio D, Hou H Jr, Kneitz B, Lagaud G, Christ GJ, Edelmann W, Lisanti MP. Caveolin-1 null mice are viable but show evidence of hyperproliferative and vascular abnormalities. *J Biol Chem*. 2001; 276:38121–38138. [PubMed: 11457855]
14. Giardiello FM, Trimpathy JD. Peutz-jeghers syndrome and management recommendations. *Clin Gastroenterol Hepatol*. 2006; 4:408–415. [PubMed: 16616343]
15. Katajisto P, Vallenius T, Vaahtomeri K, Ekman N, Udd L, Tiainen M, Makela TP. The LKB1 tumor suppressor kinase in human disease. *Biochim Biophys Acta*. 2007; 1775:63–75. [PubMed: 17010524]
16. Alessi DR, Sakamoto K, Bayascas JR. LKB1-dependent signaling pathways. *Annu Rev Biochem*. 2006; 75:137–163. [PubMed: 16756488]
17. Shackelford DB, Shaw RJ. The LKB1-AMPK pathway: Metabolism and growth control in tumour suppression. *Nat Rev Cancer*. 2009; 9:563–575. [PubMed: 19629071]
18. Ylikorkala A, Rossi DJ, Korsisaari N, Luukko K, Alitalo K, Henkemeyer M, Mäkelä TP. Vascular abnormalities and deregulation of vegf in LKB1-deficient mice. *Science*. 2001; 293:1323–1326. [PubMed: 11509733]
19. Londesborough A, Vaahtomeri K, Tiainen M, Katajisto P, Ekman N, Vallenius T, Mäkelä TP. LKB1 in endothelial cells is required for angiogenesis and TGFbeta-mediated vascular smooth muscle cell recruitment. *Development*. 2008; 135:2331–2338. [PubMed: 18539926]
20. Ohashi K, Ouchi N, Higuchi A, Shaw RJ, Walsh K. LKB1 deficiency in Tie2-cre-expressing cells impairs ischemia-induced angiogenesis. *J Biol Chem*. 2010; 285:22291–22298. [PubMed: 20489196]
21. Gustafsson E, Brakebusch C, Hietanen K, Fassler R. Tie-1-directed expression of cre recombinase in endothelial cells of embryoid bodies and transgenic mice. *J Cell Sci*. 2001; 114:671–676. [PubMed: 11171372]
22. Kisanuki YY, Hammer RE, Miyazaki J, Williams SC, Richardson JA, Yanagisawa M. Tie2-cre transgenic mice: A new model for endothelial cell-lineage analysis in vivo. *Dev Biol*. 2001; 230:230–242. [PubMed: 11161575]
23. Alva JA, Zovein AC, Monvoisin A, Murphy T, Salazar A, Harvey NL, Carmeliet P, Iruela-Arispe ML. VE-Cadherin-Cre-recombinase transgenic mouse: A tool for lineage analysis and gene deletion in endothelial cells. *Dev Dyn*. 2006; 235:759–767. [PubMed: 16450386]
24. Bardeesy N, Sinha M, Hezel AF, Signoretti S, Hathaway NA, Sharpless NE, Loda M, Carrasco DR, DePinho RA. Loss of the LKB1 tumour suppressor provokes intestinal polyposis but resistance to transformation. *Nature*. 2002; 419:162–167. [PubMed: 12226664]
25. Zhang W, Wang Q, Song P, Zou MH. Liver kinase B1 is required for white adipose tissue growth and differentiation. *Diabetes*. 2013; 62:2347–2358. [PubMed: 23396401]
26. Liang B, Wang S, Wang Q, Zhang W, Viollet B, Zhu Y, Zou MH. Aberrant endoplasmic reticulum stress in vascular smooth muscle increases vascular contractility and blood pressure in mice deficient of AMP-activated protein kinase- $\alpha$ 2 in vivo. *Arterioscler Thromb Vasc Biol*. 2013; 33:595–604. [PubMed: 23288166]

27. García-Cardena G, Fan R, Stern DF, Liu J, Sessa WC. Endothelial nitric oxide synthase is regulated by tyrosine phosphorylation and interacts with caveolin-1. *J Biol Chem.* 1996; 271:27237–27240. [PubMed: 8910295]
28. Feron O, Belhassen L, Kobzik L, Smith TW, Kelly RA, Michel T. Endothelial nitric oxide synthase targeting to caveolae. Specific interactions with caveolin isoforms in cardiac myocytes and endothelial cells. *J Biol Chem.* 1996; 271:22810–22814. [PubMed: 8798458]
29. Wang W, Fan J, Yang X, Fürer-Galban S, Lopez de Silanes I, von Kobbe C, Guo J, Georas SN, Fougelle F, Hardie DG, Carling D, Gorospe M. AMP-activated kinase regulates cytoplasmic HuR. *Mol Cell Biol.* 2002; 22:3425–3436. [PubMed: 11971974]
30. Lee S, Chen TT, Barber CL, Jordan MC, Murdock J, Desai S, Ferrara N, Nagy A, Roos KP, Iruela-Arispe ML. Autocrine VEGF signaling is required for vascular homeostasis. *Cell.* 2007; 130:691–703. [PubMed: 17719546]
31. Goetz JG, Lajoie P, Wiseman SM, Nabi IR. Caveolin-1 in tumor progression: The good, the bad and the ugly. *Cancer Metastasis Rev.* 2008; 27:715–735. [PubMed: 18506396]
32. Xie Z, Dong Y, Zhang M, Cui MZ, Cohen RA, Riek U, Neumann D, Schlattner U, Zou MH. Activation of protein kinase C zeta by peroxynitrite regulates LKB1-dependent AMP-activated protein kinase in cultured endothelial cells. *J Biol Chem.* 2006; 281:6366–75. [PubMed: 16407220]
33. Xie Z, Dong Y, Scholz R, Neumann D, Zou MH. Phosphorylation of LKB1 at serine 428 by protein kinase C-zeta is required for metformin-enhanced activation of the AMP-activated protein kinase in endothelial cells. *Circulation.* 2008; 117:952–62. [PubMed: 18250273]
34. Levy NS, Chung S, Furneaux H, Levy AP. Hypoxic stabilization of vascular endothelial growth factor mRNA by the RNA-binding protein HuR. *J Biol Chem.* 1998; 273:6417–6423. [PubMed: 9497373]
35. Wang W, Furneaux H, Cheng H, Caldwell MC, Hutter D, Liu Y, Holbrook N, Gorospe M. HuR regulates p21 mRNA stabilization by ultraviolet light. *Mol Cell Biol.* 2000; 20:760–769. [PubMed: 10629032]
36. Maurer F, Tierney M, Medcalf RL. An AU-rich sequence in the 3'-UTR of plasminogen activator inhibitor type 2 (PAI-2) mRNA promotes PAI-2 mRNA decay and provides a binding site for nuclear HuR. *Nucleic Acids Res.* 1999; 27:1664–1673. [PubMed: 10075998]
37. Schubert W, Frank PG, Woodman SE, Hyogo H, Cohen DE, Chow CW, Lisanti MP. Microvascular hyperpermeability in caveolin-1(–/–) knock-out mice. Treatment with a specific nitric-oxide synthase inhibitor, L-NAME, restores normal microvascular permeability in Cav-1 null mice. *J Biol Chem.* 2002; 277:40091–40098. [PubMed: 12167625]
38. Fernández-Hernando C, Yu J, Suarez Y, Rahner C, Davalos A, Lasuncion MA, Sessa WC. Genetic evidence supporting a critical role of endothelial caveolin-1 during the progression of atherosclerosis. *Cell Metab.* 2009; 10:48–54. [PubMed: 19583953]
39. Chidlow JH Jr, Greer JJ, Anthoni C, Bernatchez P, Fernandez-Hernando C, Bruce M, Abdelbaqi M, Shukla D, Granger DN, Sessa WC, Kevil CG. Endothelial caveolin-1 regulates pathologic angiogenesis in a mouse model of colitis. *Gastroenterology.* 2009; 136:575–584. [PubMed: 19111727]
40. Reihill JA, Ewart MA, Hardie DG, Salt IP. AMP-activated protein kinase mediates VEGF-stimulated endothelial no production. *Biochem Biophys Res Commun.* 2007; 354:1084–1088. [PubMed: 17276402]
41. Davis BJ, Xie Z, Viollet B, Zou MH. Activation of the AMP-activated kinase by antidiabetes drug metformin stimulates nitric oxide synthesis in vivo by promoting the association of heat shock protein 90 and endothelial nitric oxide synthase. *Diabetes.* 2006; 55:496–505. [PubMed: 16443786]
42. Cheng KK, Lam KS, Wang Y, Huang Y, Carling D, Wu D, Wong C, Xu A. Adiponectin-induced endothelial nitric oxide synthase activation and nitric oxide production are mediated by APPL1 in endothelial cells. *Diabetes.* 2007; 56:1387–1394. [PubMed: 17287464]
43. Fisslthaler B, Fleming I. Activation and signaling by the AMP-activated protein kinase in endothelial cells. *Circ Res.* 2009; 105:114–127. [PubMed: 19608989]

44. Nagata D, Mogi M, Walsh K. AMP-activated protein kinase (AMPK) signaling in endothelial cells is essential for angiogenesis in response to hypoxic stress. *J Biol Chem.* 2003; 278:31000–31006. [PubMed: 12788940]
45. Noga AA, Soltys CL, Barr AJ, Kovacic S, Lopaschuk GD, Dyck JR. Expression of an active LKB1 complex in cardiac myocytes results in decreased protein synthesis associated with phenylephrine-induced hypertrophy. *Am J Physiol Heart Circ Physiol.* 2007; 292:H1460–1469. [PubMed: 17098823]
46. Calamaras TD, Lee C, Lan F, Ido Y, Siwik DA, Colucci WS. Post-translational modification of serine/threonine kinase LKB1 via adduction of the reactive lipid species 4-hydroxy-trans-2-nonenal (HNE) at lysine residue 97 directly inhibits kinase activity. *J Biol Chem.* 2012; 287:42400–42406. [PubMed: 23086944]

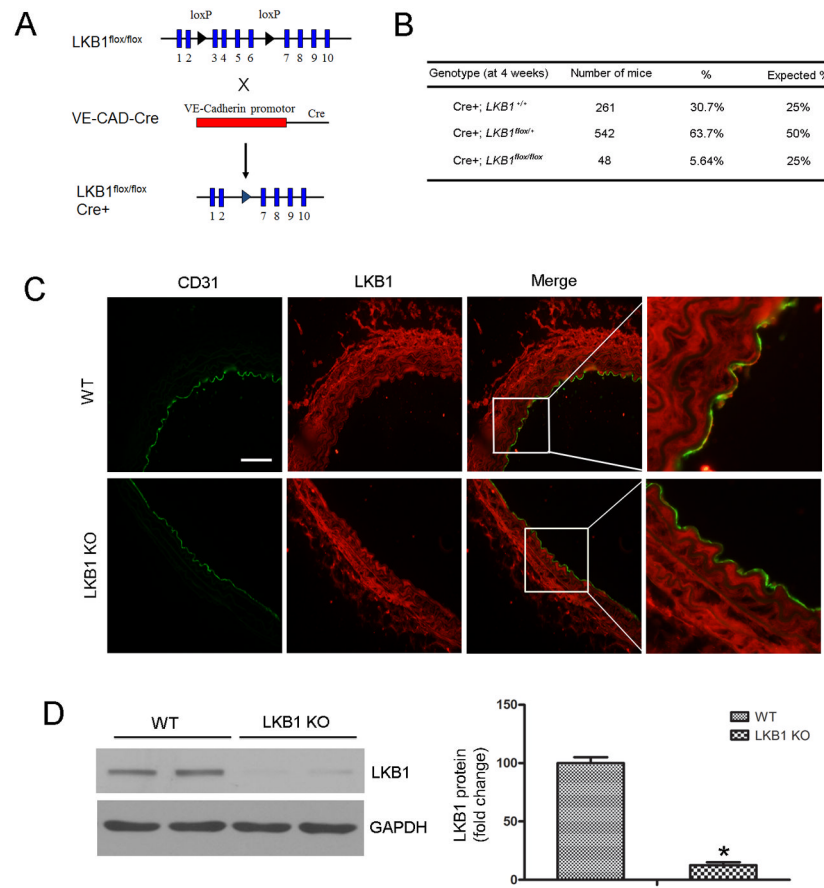


**Figure 1.** Generation and characterization of *LKB1*<sup>endo-/-</sup> mice. **A**, Schematic diagram of the transgenic mice used to generate *LKB1*<sup>endo-/-</sup> mice. **B**, Genotyping analysis of 4-week old mice. VE-CAD-Cre/*LKB1*<sup>fllox/+</sup> mice were inter-bred. A total of 851 mice from 40 litters were genotyped. **C**, Immunostaining to determine LKB1 (red) and CD31 (green) localization in aortic sections from *LKB1*<sup>endo-/-</sup> and WT mice. Scale bar = 50  $\mu$ m. **D**, Western blot analysis to detect LKB1 expression in WT and LKB1-deficient MLECs (n = 4). \*p < 0.05 vs. WT.



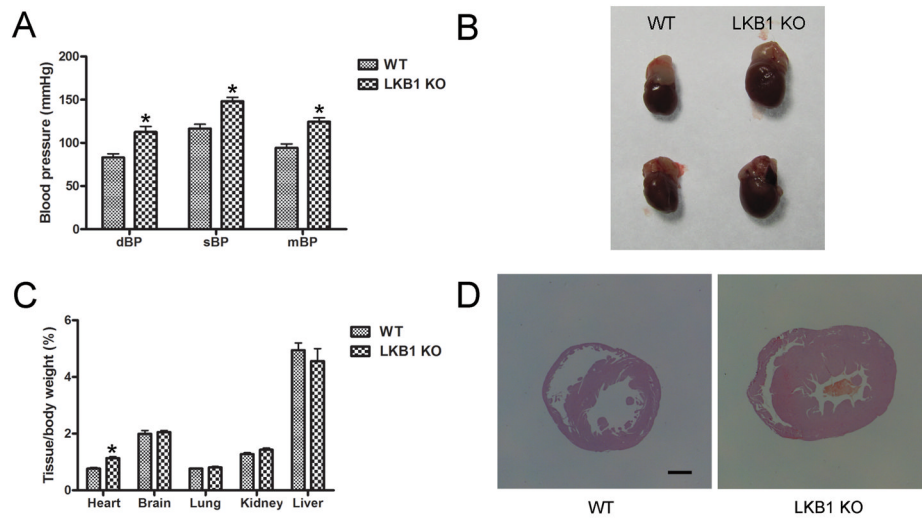


**Figure 2.** Elevated blood pressure and cardiac hypertrophy in *LKB1<sup>endo-/-</sup>* mice. **A**, Blood pressure from male WT and *LKB1<sup>endo-/-</sup>* mice at three months was measured using the radiotelemetry technique (n = 10). **B**, Appearance of hearts from WT and *LKB1<sup>endo-/-</sup>* mice. **C**, Weight of various organs relative to overall body weight in WT and *LKB1<sup>endo-/-</sup>* mice (n = 5). **D**, Hearts from WT and *LKB1<sup>endo-/-</sup>* mice were stained with hematoxylin and eosin (H&E). Scale bar = 1 mm. \*p < 0.05 vs. WT.

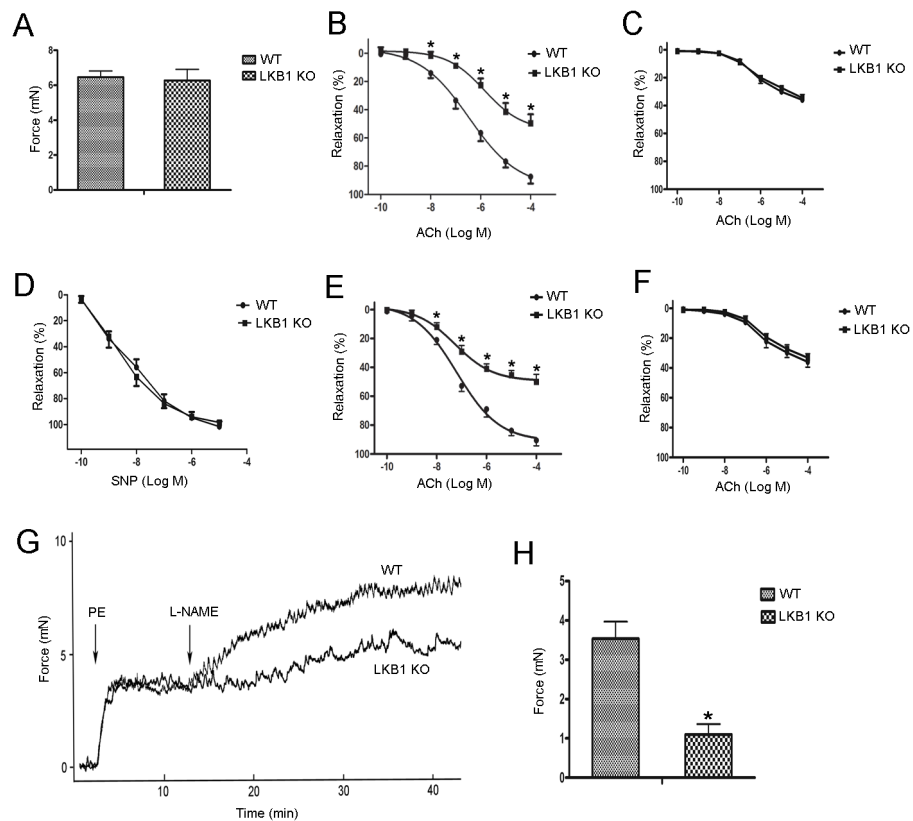


**Figure 3.** Endothelial deletion of LKB1 impairs eNOS-dependent vasodilation. **A**, PE-induced contraction force in aortic rings from *LKB1<sup>endo-/-</sup>* and WT mice. Vascular reactivity of *LKB1<sup>endo-/-</sup>* and WT aortic rings to ACh without (**B**) or with L-NAME pretreatment (100  $\mu$ M) for 30 min (**C**). **D**, Vascular reactivity of *LKB1<sup>endo-/-</sup>* and WT aortic rings to SNP. Vascular reactivity of *LKB1<sup>endo-/-</sup>* and WT mesenteric vessels to ACh without (**E**) or with L-NAME pretreatment (**F**). Aortic rings from *LKB1<sup>endo-/-</sup>* and WT mice were contracted with PE (10<sup>-7</sup> M) and then incubated with L-NAME (100  $\mu$ M) to remove basal NO synthesis. A representative contraction curve is shown (**G**) and the force (**H**) was quantified. Data are mean  $\pm$  SEM, n = 5 animals and two aortic rings per animal. \*p < 0.05 vs. WT.

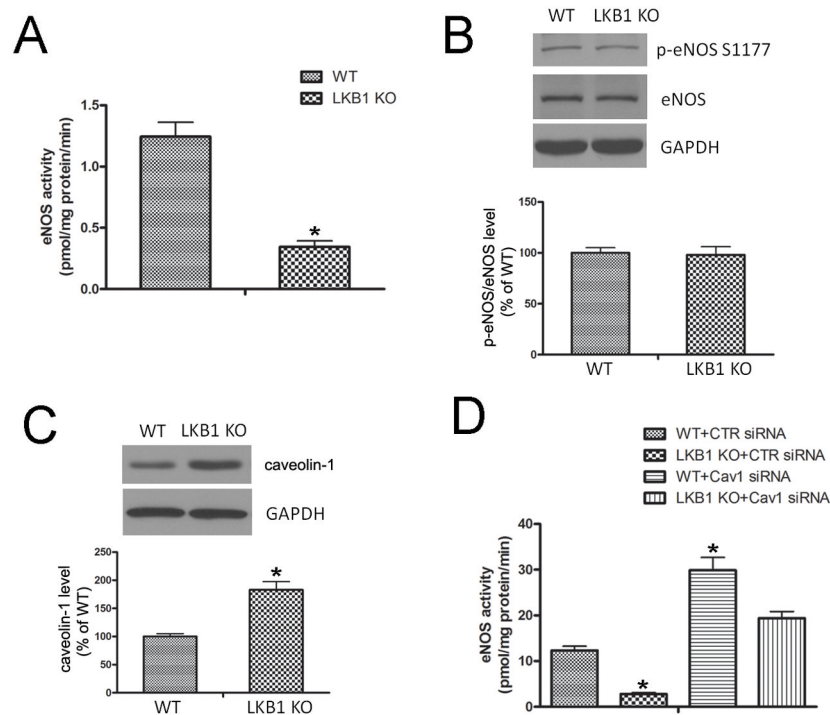


**Figure 4.** Decreased eNOS activity in *LKB1<sup>endo-/-</sup>* mice. **A**, eNOS activity from WT or *LKB1<sup>endo-/-</sup>* lung extracts was measured according to [<sup>3</sup>H] arginine-to-citrulline conversion (n = 5). \*p < 0.05 vs. WT. Western blot detection of phosphorylated eNOS at Ser1177 (**B**) and caveolin-1 (**C**) in MLECs from WT or *LKB1<sup>endo-/-</sup>* mice (n = 4). \*p < 0.05 vs. WT. **D**, eNOS activity was monitored in WT or LKB1-deficient MLECs transfected with control (CTR) siRNA or caveolin-1 siRNA (n = 4). \*p < 0.05 vs. WT+CTR siRNA.

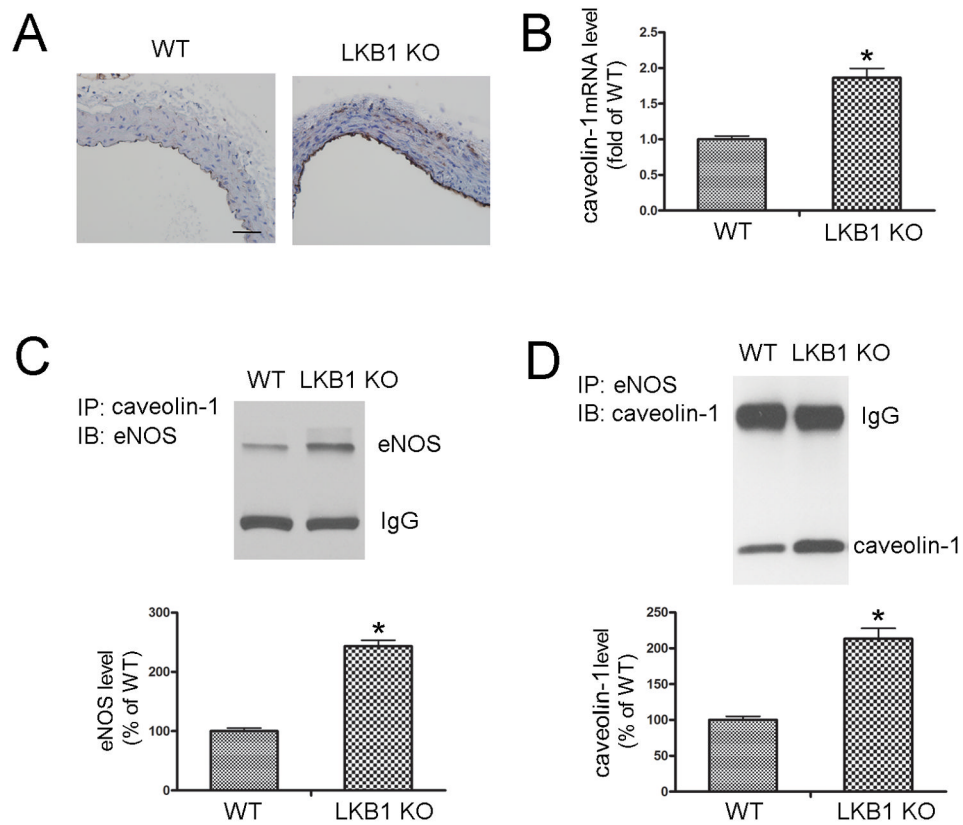


**Figure 5.** Increased expression of caveolin-1 in the endothelium of *LKB1<sup>endo-/-</sup>* mice. **A**, Immunohistochemical staining for caveolin-1 in aortas from WT and *LKB1<sup>endo-/-</sup>* mice. Scale bar = 50  $\mu$ m. **B**, RT-PCR to detect caveolin-1 mRNA levels in MLECs from WT and *LKB1<sup>endo-/-</sup>* mice (n = 4). Caveolin-1 (**C**) or eNOS (**D**) was immunoprecipitated from WT or *LKB1<sup>endo-/-</sup>* lung lysates, and eNOS or caveolin-1 in the immunoprecipitates was detected by western blot (n = 5). \*p < 0.05 vs. WT.

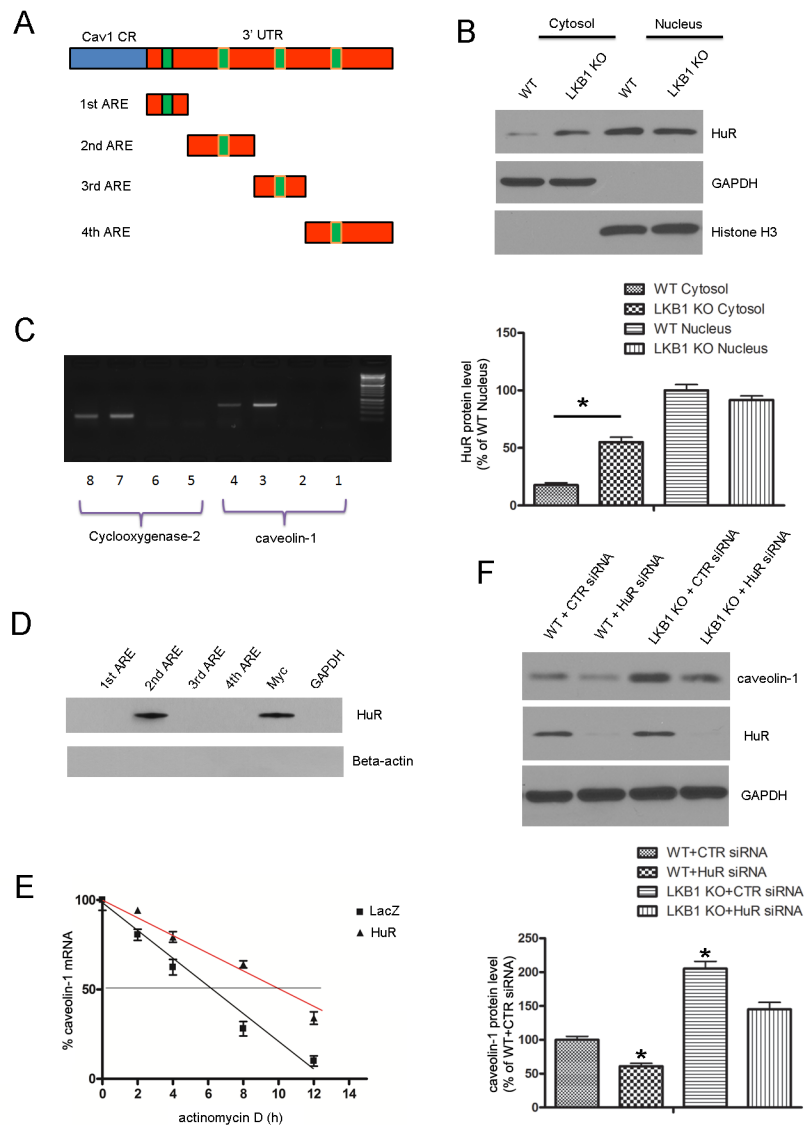


**Figure 6.** Caveolin-1 is a target of HuR. **A**, The schematic representations of predicted AU-rich elements (AREs) in the 3'UTR of caveolin-1 mRNA are depicted, along with the RNA probes that were used in the RNA pull-down assay. **B**, Cytoplasmic and nuclear fractions were isolated from WT and LKB1-deficient endothelial cells, followed by immunoblotting to detect HuR (n = 4). \*p < 0.05 vs. WT Cytosol. **C**, RNA immunoprecipitation (IP) was carried out with the anti-HuR antibody or with the control IgG. Cyclooxygenase-2 was used as the positive control in this assay. Lanes 1 & 5: No template PCR control. Lanes 2 & 6: IgG RNA IP. Lanes 3 & 7: Anti-HuR RNA IP. Lanes 4 & 8: 10% Input. **D**, Proteins that were pulled down with biotinylated RNA probes corresponding to different AREs in the 3'UTR of caveolin-1 mRNA, 3'UTR of Myc (positive control), or 3'UTR of GAPDH (negative control) were visualized by immunoblotting, using the HuR antibody. **E**, Endothelial cells were transfected with LacZ or HuR plasmid, and then treated with actinomycin D (5  $\mu$ g/ml). The levels of caveolin-1 mRNA were determined by RT-PCR (n = 4). **F**, MLECs from WT and *LKB1*<sup>endo-/-</sup> mice were transfected with control or HuR-



specific siRNA for 48 h, followed by Western blot analysis to detect caveolin-1 (n = 4). \*p < 0.05 vs. WT+CTR siRNA.

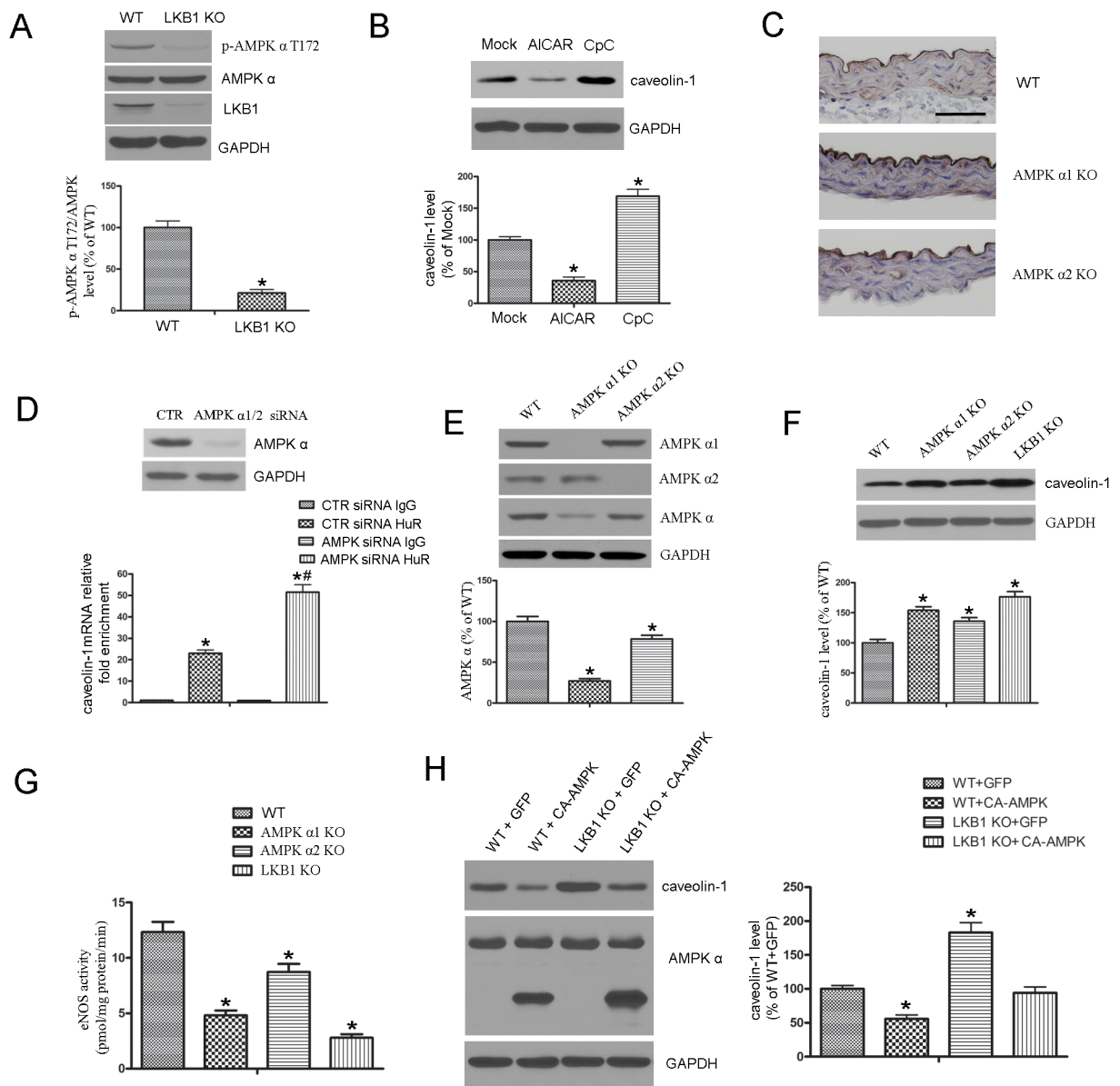


**Figure 7.**

LKB1 regulates caveolin-1 expression in an AMPK-dependent manner. **A**, Western blot analysis of p-AMPK $\alpha$  (T172) in MLECs from WT or *LKB1*<sup>endo-/-</sup> mice. \* $p < 0.05$  vs. WT. **B**, WT MLECs were treated with AICAR (2 mM) or Compound C (CpC; 20  $\mu$ M) for 48 hours, followed by Western blot analysis (n = 4). \* $p < 0.05$  vs. Mock. **C**, Immunostaining for caveolin-1 in aortas from WT, *AMPK $\alpha$ 1*<sup>-/-</sup>, and *AMPK $\alpha$ 2*<sup>-/-</sup> mice. Scale bar = 50  $\mu$ m. **D**, MLECs were transfected with control (CTR) siRNA or AMPK $\alpha$ 1/2-specific siRNA, followed by RNA immunoprecipitation (IP) with the anti-HuR antibody or control IgG. Caveolin-1 mRNA levels in each immunoprecipitate was determined by RT-PCR. Results are presented as the relative enrichment in HuR RNA IP compared to IgG RNA IP. n = 4, \* $p < 0.05$  vs. CTR siRNA IgG. # $p < 0.05$  vs. CTR siRNA HuR. **E**, MLECs from *AMPK $\alpha$ 1*<sup>-/-</sup> and *AMPK $\alpha$ 2*<sup>-/-</sup> mice were subjected to western blot analysis to detect AMPK $\alpha$  levels (n = 4). \* $p < 0.05$  vs. WT. Western blot analysis of caveolin-1 levels (**F**) and eNOS activity measurement (**G**) in MLECs from WT, *AMPK $\alpha$* <sup>-/-</sup>, and *LKB1*<sup>endo-/-</sup> mice (n = 4). \* $p < 0.05$

vs. WT. **H**, WT or LKB1-deficient MLECs were infected with constitutively active (CA)-AMPK or the control GFP virus for 48 h, followed by Western blot analysis (n = 4). \*p < 0.05 vs. WT+GFP.

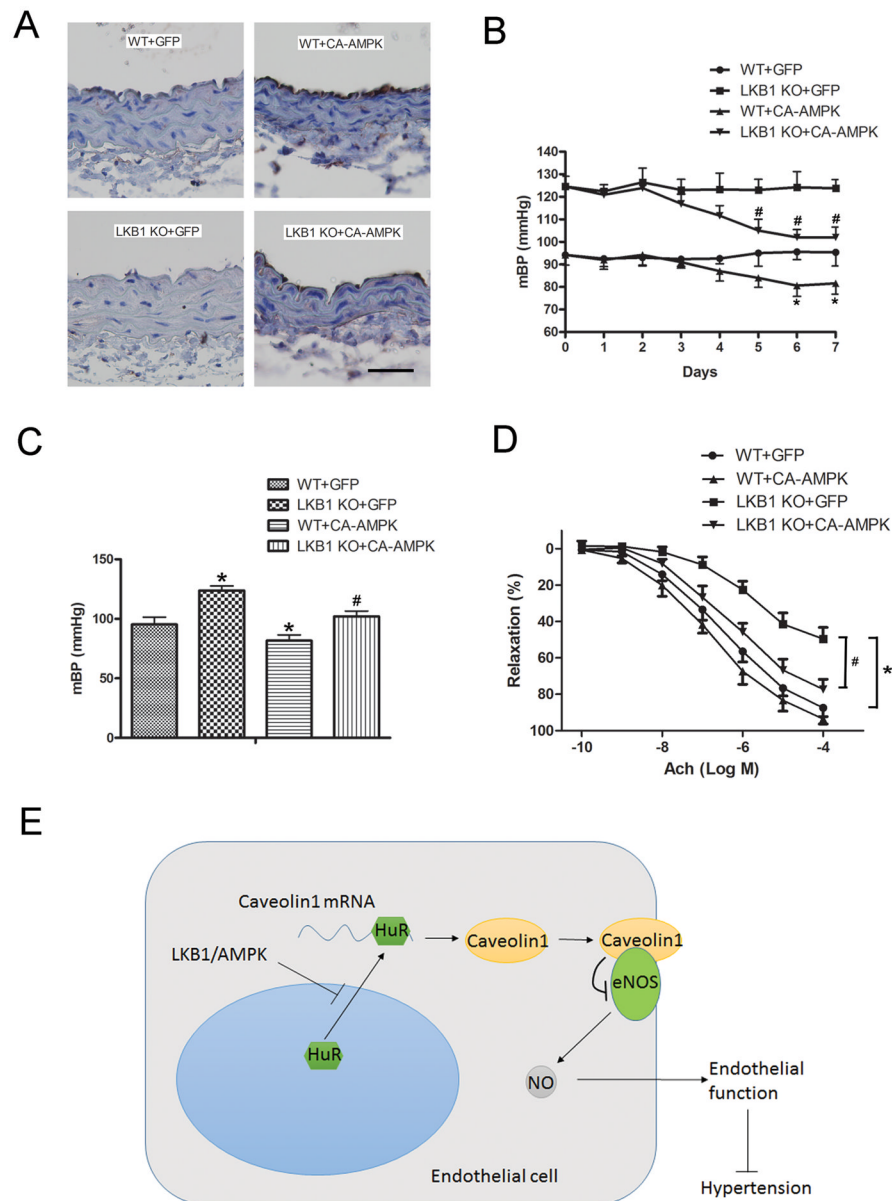


**Figure 8.** Administration of CA-AMPK alleviates endothelial dysfunction and lowers high blood pressure in *LKB1<sup>endo-/-</sup>* mice. **A**, WT or *LKB1<sup>endo-/-</sup>* mice received tail vein injections of 100  $\mu$ L adenoviral solutions that expressed GFP or CA-AMPK ( $4 \times 10^{10}$  viral particles) ( $n = 6$  in each group). After 7 days, immunohistochemical staining for p-AMPK $\alpha$  (T172) in aortas was performed. Scale bar = 50  $\mu$ m. Blood pressure from WT and *LKB1<sup>endo-/-</sup>* mice after adenoviral injections was monitored by the radiotelemetry technique, **(B)** and mean blood pressure was quantified after 7 days of injection **(C)**. \* $p < 0.05$  vs. WT+GFP; # $p < 0.05$  vs. *LKB1<sup>endo-/-</sup>*+GFP. **D**, ACh-induced vascular reactivity of aortic rings from *LKB1<sup>endo-/-</sup>* and WT mice after 7 days of injection ( $n = 6$ ). \* $p < 0.05$  vs. WT+GFP; # $p < 0.05$  vs. *LKB1<sup>endo-/-</sup>*+GFP. **E**, Diagram for LKB1-regulated eNOS activity and endothelial function through caveolin-1.